

Last Glacial Maximum cooling induced positive moisture balance and maintained stable human populations in Australia

Haidee Cadd ^{1,2,3✉}, Alan N. Williams^{4,5}, Wanchese M. Saktura ^{1,3}, Tim J. Cohen ^{1,3}, Scott D. Mooney ⁶, Chengfei He ⁷, Bette Otto-Bliesner ⁸ & Chris S. M. Turney^{2,4,9}

Long-standing interpretations of the Last Glacial Maximum (21,000 ± 2000 years ago) in Australia suggest that the period was extremely cold and arid, during which the Indo-Australian summer monsoon system collapsed, and human populations declined and retreated to ecological refuges to survive. Here, we use transient iTRACE simulations, combined with palaeoclimate proxy records and archaeological data to re-interpret the late Last Glacial Maximum and terminal Pleistocene (21,000 – 11,000 years) in Australia. The model suggests climates during the peak Last Glacial Maximum were cooler than present (–4 to –11 °C), but there is no evidence of monsoon collapse or substantial decreases in moisture balance across Australia. Kernel Density Estimates of archaeological ages show relatively stable and persistent human activity across most regions throughout the late Last Glacial Maximum and terminal Pleistocene, consistent with genetic evidence. Spatial coverage of archaeological sites steadily increased across the terminal Pleistocene; however, substantial population change is not evident.

¹ARC Centre of Excellence for Australian Biodiversity and Heritage, University of Wollongong, Wollongong, NSW, Australia. ²Chronos 14Carbon-Cycle Facility, Mark Wainwright Analytical Centre, University of New South Wales, Sydney, NSW, Australia. ³GeoQuEST Research Centre, School of Earth, Atmospheric and Life Sciences, University of Wollongong, Wollongong, NSW, Australia. ⁴ARC Centre of Excellence for Australian Biodiversity and Heritage, School of Biological Earth and Environmental Sciences, University of New South Wales, Sydney, NSW, Australia. ⁵EMM Consulting Pty Limited, 20 Chandos Street, St Leonards, NSW 2065, Australia. ⁶School of Biological Earth and Environmental Sciences, University of New South Wales, Sydney, NSW, Australia. ⁷Rosenstiel School of Marine, Atmospheric, and Earth Science, University of Miami, Miami, FL, USA. ⁸Climate and Global Dynamics Laboratory, National Center for Atmospheric Research, Boulder, CO, USA. ⁹Institute of Sustainable Futures, Division of Research, University of Technology Sydney, Sydney, NSW 2007, Australia. ✉email: haidee@uow.edu.au

Past major climatic changes and their environmental impacts provide valuable insights into how the Earth system operates under a range of boundary conditions. One key period in this regard is the Last Glacial Maximum (LGM; 23 – 19 ka), which has previously been characterised as significantly cooler and drier than present day in Australia^{1–4}. However, consensus on how the climates of Australia, the driest inhabited continent on Earth, changed during the LGM has been difficult to establish. Importantly, despite 60 years of research, the environmental and societal impacts of the LGM period have never been fully defined spatially or temporally. This is in part due to the large size of the continent (~7.7 million km²) and the numerous environments that have limited potential for preserving palaeoclimate records. Sedimentary sequences recording evidence of desiccation, depositional hiatuses and/or low sedimentation rates^{5–9} and records of vegetation change to herb and grass dominated ecosystems^{8–13} have driven the interpretation of a cool and arid environment. However, isotopic evidence for increased moisture from speleothem records^{14,15} and discontinuous records of fluvial discharge and lake high stands dated to the LGM period have challenged this hypothesis^{16–25}.

Alongside these conflicting hydroclimate states, increasingly advanced techniques applied to a growing number of palaeoclimate records is revealing considerable complexity during the LGM^{5,14,26,27}. Cadd et al.⁵ recently demonstrated that the LGM period in Australia was represented by an extended period of extreme environmental conditions from 28.6 (± 2.8) – 17.7 (± 2.2) ka, with evidence of multi-stage changes recorded in some high-resolution records. Records of sparser arboreal vegetation during this time have previously been interpreted as a sign of increased aridity^{8–13,28}, however, more recently, changes in CO₂ have been suggested as a key driver of changes between woody and non-woody vegetation types^{29,30}. The substantial declines in CO₂ during the LGM (185 ppm compared to pre-industrial values of 280 ppm) would have reduced the water-use efficiency and resilience of vegetation, resulting in lower productivity and cover, even without a reduction of hydrological supply^{30–33}. Examining the influence of landscape scale moisture balance and effective precipitation in maintaining vegetation communities and hydrological systems may help to interpret contradictory disparate proxy records³³.

The interpretation of a hyper-arid and cold LGM has in part guided the interpretation of the Australian archaeological record^{34–37}. Early work hypothesised that populations withdrew to macro-ecological refugia – generally on the fringes of the continent – with regions of the arid centre forming barriers to survival and occupation^{34,37}. However, a growing amount of data and higher resolution analyses have resulted in revisions of this previously accepted model³⁸. Demographic studies show that Aboriginal

populations only appear to reach their lowest point after the LGM period (~18ka)³⁹, with no major population changes during the preceding 10,000 years, despite the longer multi-phase characteristics of this period now becoming apparent^{5,40}. In addition, not all archaeological sites that contain material culture from this temporal period indicate abandonment⁴¹, while genomic research has not identified bottlenecks or extinctions that reflect substantive population losses^{42–44}.

In contrast to the LGM, the terminal Pleistocene (17–11ka) has been relatively under-studied in Australia, yet this period experienced a range of hydroclimate extremes, including the Antarctic Cold Reversal (ACR; 14.7–13.0 ka). The influence of ACR has been identified in proxy records in other regions of the Southern Hemisphere⁴⁵, yet evidence of a climatic expression of the ACR in Australia is rare^{1,45–48}. The limited available information regarding the terminal Pleistocene further hampers understanding of how extreme climates of the LGM were, and how human societies adapted to changing landscapes during the transition from the LGM to the Holocene⁴⁹.

There is a need for quantified climate reconstructions covering the LGM and terminal Pleistocene from Australia. Spatially disparate quantitative measures of LGM temperatures are limited and localised^{3,50–52}; and no quantitative precipitation records exist for continental Australia. Interpretations of the majority of available proxy records, largely palynological records, are confounded by multiple biophysical interactions, making climate inferences challenging^{5,29}. Here we examine iTRACE modelled temperature, precipitation and moisture balance (precipitation minus evaporation; P-E) supported by palaeoclimate proxy records to provide a record of the late LGM and terminal Pleistocene climates of Australia. We use these data to evaluate long-standing environmental and archaeological hypotheses.

Results and discussion

For this study we utilised the iTRACE that simulates the deglacial temperature, precipitation and evaporation, supported by palaeoclimate proxy records (see Supplement for Methods). It must be noted that the iTRACE is a single model simulation and therefore some aspects of the model results, such as the hydrological cycle, may be model dependent⁵³. However, the coherence observed between rainfall-derived changes in $\delta^{18}\text{O}$ of calcite in Australian speleothem records and modelled precipitation suggests the iTRACE precipitation output can accurately reconstruct past precipitation patterns for Australia. Pre-industrial simulation from the iCESM1.3 model, the same model version as iTRACE, shows similar patterns to modern Australian temperature and

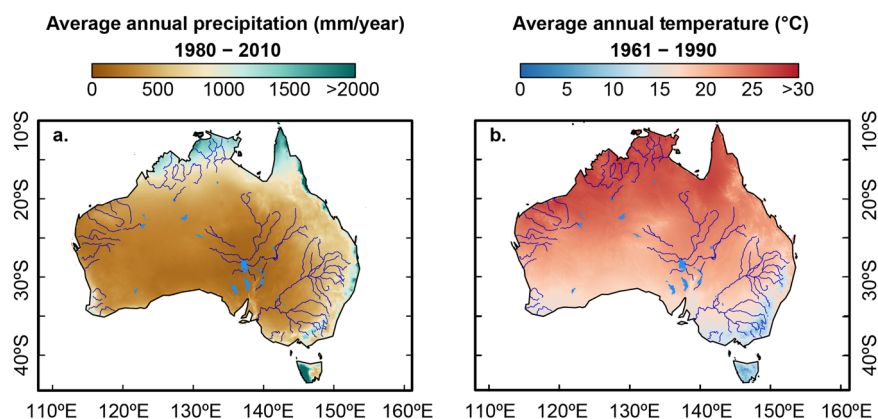


Fig. 1 Modern average annual precipitation and temperature for Australia. Average annual precipitation (a) and temperature (b) across Australia. Major river systems and lakes are shown in blue. Data from Australian Gridded Climate Dataset (AGCD) from Bureau of Meteorology (BOM)⁸⁷.

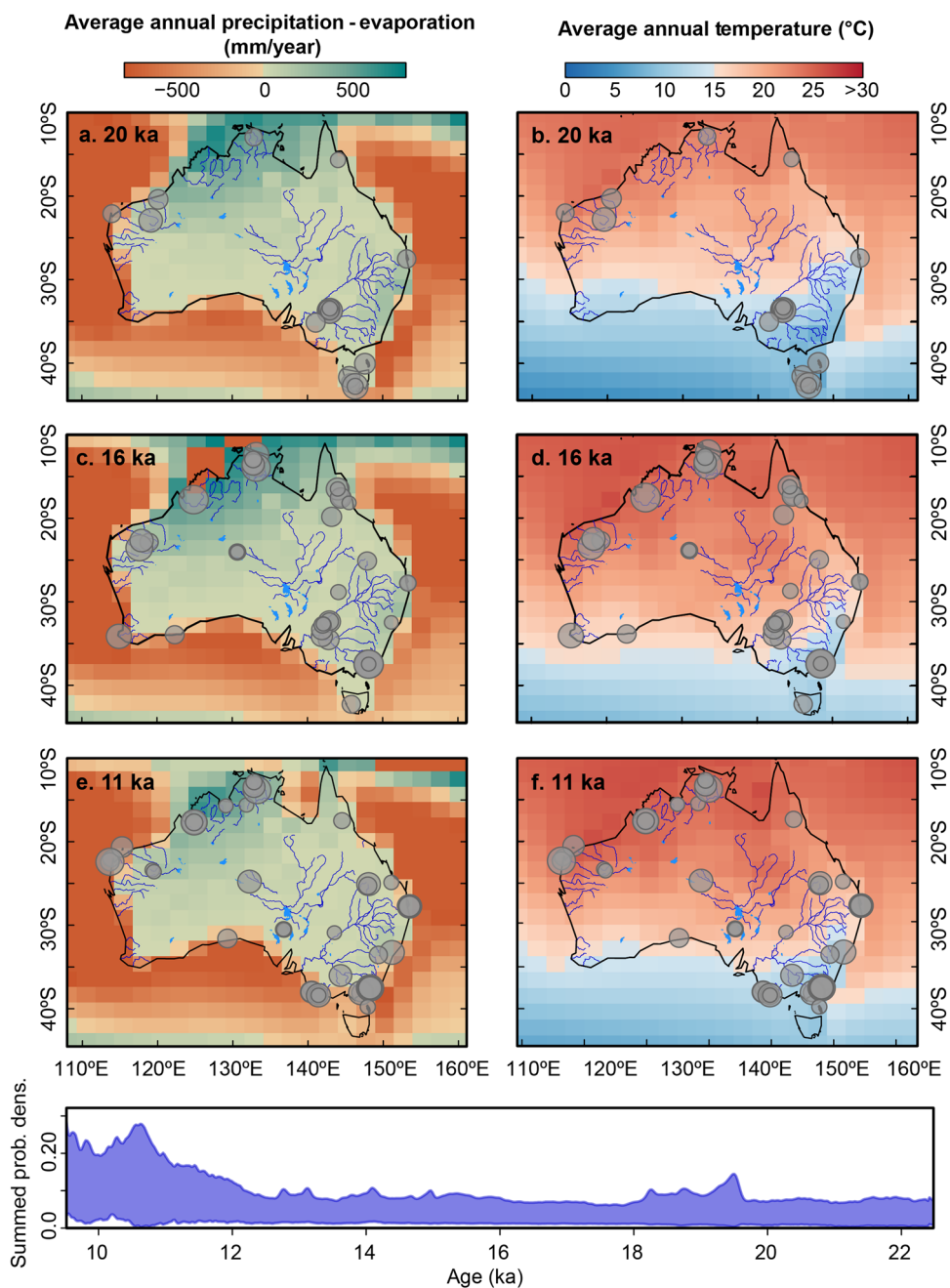


Fig. 2 iTRACE average annual moisture balance and temperature with Kernel Density Estimate of Archaeological ages. iTRACE average annual precipitation minus evaporation (P-E) (a, c, e) and average annual temperature (b, d, f) at 20, 16 and 11 ka. The location of ages from archaeological sites (radiocarbon, OSL & TL) that had a probability >0.01 of occurring ± 200 years of each time slice are plotted as grey circles. Size of circles is proportional to probability of occurrence. Bottom panel shows a Gaussian KDE (bandwidth=30) of archaeological ages (radiocarbon, OSL & TL) through time. Archaeological ages were extracted from the SahulArch database v.2. Major river systems and lakes are shown in blue.

rainfall, further increasing confidence in the model simulations. The fidelity of the precipitation outputs from the iTRACE have previously been documented for regions north of Australia, including the Sunda shelf^{54,55}.

At a continental scale, the iTRACE data indicates that average annual continental temperature at 20 ka were 4 – 11 °C cooler than present (Fig. 1, Fig. 2; Table 1). These cooler conditions are maintained throughout the terminal Pleistocene, with all latitudes progressively becoming warmer after 17 ka (Fig. 2, Fig. 3; Table 1). Average annual temperatures for latitudes below 30°S experience the greatest declines, with temperatures up to 11 °C below present during the LGM. Temperatures south of 30°S did

not exceed 17 °C until 12.5 ka, whilst regions above 20°S remained above 20 °C throughout the LGM and terminal Pleistocene. In both regions temperatures were cooler than present day, but would have been a reasonable thermal comfort level for Indigenous populations. A reversal of ~ 1.5 °C in the warming temperature trend is evident during the ACR between 14.4 and 13.9 ka.

Modelled precipitation minus evaporation (P-E) trends are both regionally and seasonally variable, with most regions reflecting a slightly positive moisture balance between 21 and 11ka (Figs. 2 and 3), similar to recent multi-model ensembles²⁷. The positive moisture balance at a continental scale is strongly

Table 1 Average iTRACE precipitation and temperature values.

	Annual		DJF		MAM		JJA		SON	
Continent	Temp (°C)	Precip (mm)								
20 ka	17.4 ± 0.1	636 ± 33	23.0 ± 0.2	329 ± 11	17.6 ± 0.2	150 ± 12	10.5 ± 0.2	63 ± 5	18.5 ± 0.1	91 ± 9
18 ka	17.3 ± 0.1	618 ± 21	22.7 ± 0.2	316 ± 12	17.5 ± 0.1	154 ± 8	10.7 ± 0.1	62 ± 4	18.3 ± 0.1	84 ± 8
16 ka	20.2 ± 0.1	713 ± 30	25.0 ± 0.1	360 ± 15	20.3 ± 0.1	179 ± 12	13.9 ± 0.1	63 ± 6	21.7 ± 0.1	107 ± 12
14 ka	20.0 ± 0.3	605 ± 68	24.5 ± 0.3	294 ± 30	19.8 ± 0.4	147 ± 13	14.1 ± 0.6	62 ± 12	21.5 ± 0.4	99 ± 17
13.5 ka	21.1 ± 0.1	642 ± 19	25.4 ± 0.2	310 ± 8	20.9 ± 0.2	157 ± 9	15.3 ± 0.1	64 ± 6	22.8 ± 0.2	104 ± 9
12.5 ka	21.4 ± 0.1	693 ± 51	25.6 ± 0.3	329 ± 19	20.9 ± 0.2	169 ± 14	15.8 ± 0.2	69 ± 9	23.3 ± 0.2	123 ± 18
11 ka	22.3 ± 0.1	663 ± 29	26.5 ± 0.2	313 ± 16	21.7 ± 0.3	157 ± 7	16.7 ± 0.2	65 ± 6	24.4 ± 0.1	125 ± 7
Present	21.5 ± 0.5	481 ± 30	27.4 ± 0.4	223 ± 25	21.7 ± 0.5	114 ± 9	14.8 ± 0.4	66 ± 5	22.2 ± 0.6	79 ± 8
North 20°	Temp (°C)	Precip (mm)								
20 ka	21.8 ± 0.2	1025 ± 48	23.7 ± 0.1	660 ± 15	21.7 ± 0.3	227 ± 36	17.4 ± 0.3	13 ± 2	24.4 ± 0.2	117 ± 8
18 ka	21.7 ± 0.1	1007 ± 37	23.4 ± 0.1	642 ± 21	21.6 ± 0.2	238 ± 16	17.8 ± 0.2	13 ± 2	24.2 ± 0.1	107 ± 13
16 ka	23.7 ± 0.1	1161 ± 41	24.7 ± 0.1	712 ± 22	23.2 ± 0.2	300 ± 21	20.3 ± 0.2	12 ± 2	26.6 ± 0.2	128 ± 16
14 ka	24.2 ± 0.3	985 ± 70	25.1 ± 0.3	604 ± 48	23.4 ± 0.2	235 ± 22	21.2 ± 0.4	13 ± 3	27.0 ± 0.3	127 ± 15
13.5 ka	25.1 ± 0.1	1011 ± 21	26.0 ± 0.1	603 ± 15	24.2 ± 0.2	254 ± 15	22.1 ± 0.2	13 ± 3	28.2 ± 0.1	129 ± 13
12.5 ka	24.9 ± 0.1	1090 ± 48	25.7 ± 0.2	629 ± 27	23.7 ± 0.2	289 ± 21	21.9 ± 0.2	16 ± 4	28.1 ± 0.3	149 ± 24
11 ka	26.1 ± 0.1	1080 ± 43	27.2 ± 0.3	612 ± 28	24.9 ± 0.2	275 ± 11	23.1 ± 0.2	16 ± 3	29.2 ± 0.1	170 ± 10
Present	26.8 ± 0.4	854 ± 45	28.7 ± 0.4	561 ± 39	26.8 ± 0.5	196 ± 13	23.9 ± 0.4	15 ± 4	28.6 ± 0.6	82 ± 8
South 30°	Temp (°C)	Precip (mm)								
20 ka	12.3 ± 0.1	483 ± 25	19.5 ± 0.2	142 ± 11	12.7 ± 0.1	125 ± 6	5.3 ± 0.2	120 ± 6	11.9 ± 0.2	95 ± 12
18 ka	12.2 ± 0.1	474 ± 23	19.2 ± 0.2	131 ± 10	12.6 ± 0.1	129 ± 10	5.3 ± 0.1	121 ± 5	11.7 ± 0.1	92 ± 5
16 ka	15.9 ± 0.1	513 ± 24	22.6 ± 0.1	146 ± 8	16.3 ± 0.1	132 ± 9	9.0 ± 0.1	126 ± 8	15.7 ± 0.1	108 ± 10
14 ka	14.9 ± 0.5	474 ± 64	21.0 ± 0.3	125 ± 12	15.2 ± 0.6	121 ± 12	8.6 ± 1.0	126 ± 23	14.9 ± 0.5	101 ± 21
13.5 ka	16.2 ± 0.1	517 ± 22	22.0 ± 0.2	137 ± 7	16.5 ± 0.1	129 ± 9	10.2 ± 0.1	134 ± 9	16.2 ± 0.2	112 ± 7
12.5 ka	17.1 ± 0.1	540 ± 43	22.8 ± 0.3	149 ± 17	17.0 ± 0.2	131 ± 12	11.1 ± 0.1	137 ± 10	17.4 ± 0.1	122 ± 12
11 ka	17.6 ± 0.2	516 ± 19	23.0 ± 0.1	149 ± 8	17.6 ± 0.3	120 ± 7	11.8 ± 0.2	133 ± 7	18.1 ± 0.2	113 ± 3
Present	23.5 ± 0.5	474 ± 22	30.2 ± 0.6	108 ± 12	23.7 ± 0.5	108 ± 9	15.7 ± 0.3	140 ± 7	24.4 ± 0.5	118 ± 9

Austral Summer, DJF December, January, February; Austral Autumn, MAM March, April May; Austral winter, JJA June, July August; Austral spring, SON September, October, November. Annual and seasonal iTRACE precipitation and temperature values for all continental grid cells, all grid cells North of 20°S latitude and all grid cells South of 30°S latitude at 20, 18, 16, 14, 13.5, 12.5 and 11ka. Each time slice represents the average and standard deviation of the decadal averages for 100 years (50 years either side of the year), except for 20 and 11ka which are a 50-year average. Present temperature and precipitation values are averaged from 1961 to 1990 average. All present data is sourced from the Bureau of Meteorology Australian Climate Observations Reference Network-Surface Air Temperature (ACORN-SAT) dataset for temperature averages and Australian Gridded Climate Data (AGCD) dataset for precipitation averages⁸⁷.

influenced by the northern latitudes (Figs. 2 and 3), likely driven by the continuation of the Indo-Australian summer monsoon (IASM) system. Continental, north of 20°S and arid – semi-arid regions display similar trends in P-E, with positive annual and positive summer P-E and negative winter and spring P-E (Fig. 3; Figs. S16–S18). The positive P-E values in the arid – semi-arid zone, defined by modern day precipitation values < 350 mm/yr, suggest either an increase in the continental penetration of the IASM or a strong influence of other tropical climate drivers, such as the Indian Ocean Dipole (IOD). The highest moisture balance in these regions occurs between 17.5 and 14.7 ka (Fig. 3).

This is in contrast to previous studies that have suggested the IASM was greatly weakened relative to today during the LGM^{56,57} and that the IASM did not ‘switch-on’ until ~13–14 ka^{58,59}. Direct evidence for a substantially weaker IASM and drier continental climates is limited. Relatively wet conditions, indicative of a strong IASM and southerly inter-tropical convergence zone (ITCZ), are recorded from ~17 – 14.7 ka in hydroclimate records from Indonesia^{60–62} and northern Australia^{15,63,64} (Fig. 4). Further, multi-model ensembles suggest a strengthening of the IASM⁶⁵ and increased monsoonal and summer precipitation in the central Australian monsoon region during the LGM⁶⁶. The wettest phase in the Mairs Cave speleothem record occurs between 18.9 and 15.8 ka and comparison with regional records indicates a tropical or sub-tropical source of this moisture¹⁴. The correspondence between the iTRACE precipitation outputs and the $\delta^{18}\text{O}$ of calcite from well-dated speleothem records suggest that the IASM was not only active during the

LGM, but penetrated farther south (Fig. 4)^{14,63} as suggested by Treble et al.¹⁴.

The P-E of southern and eastern regions record similar trends, with an overall declining trend from 20 to 11 ka (Figs. 2 and 3) and negative annual P-E south of 30°S from 20 to 11ka and from 14 to 11ka on the east coast. The changes in moisture balance and precipitation in the region south of 30°S are primarily seasonal, with summer and autumn rainfall higher than present day values, while winter and spring rainfall are lower (Fig. S19, Table 1). The reduction in winter and spring rainfall may suggest a southward contraction or reduced strength of the Southern Westerly Winds (SWW), resulting in reduced winter and spring precipitation in southern Australia⁶⁷.

Palynological records that document a reduction in woody and arboreal vegetation have widely been used as an indicator for substantial decreases in precipitation during the LGM^{8–13}. This is in contrast to discontinuous records that suggest increased hydrological activity and enhanced surface run-off^{16–24}. The preservation of fluvial geomorphic features representing increased discharge and lake-full conditions in the Murray-Darling Basin (MDB) and Lake Eyre Basin (LEB), Australia’s two largest drainage basins, during the LGM and terminal Pleistocene suggest these hydrological systems were not substantially reduced during this period (Fig. 4; Fig. S4). The integration of the disparate proxy records, along with and iTRACE allows these contradictory proxy records to be fully interrogated.

The low levels of arboreal vegetation during the LGM have been hypothesised to have occurred as a response to low CO₂,

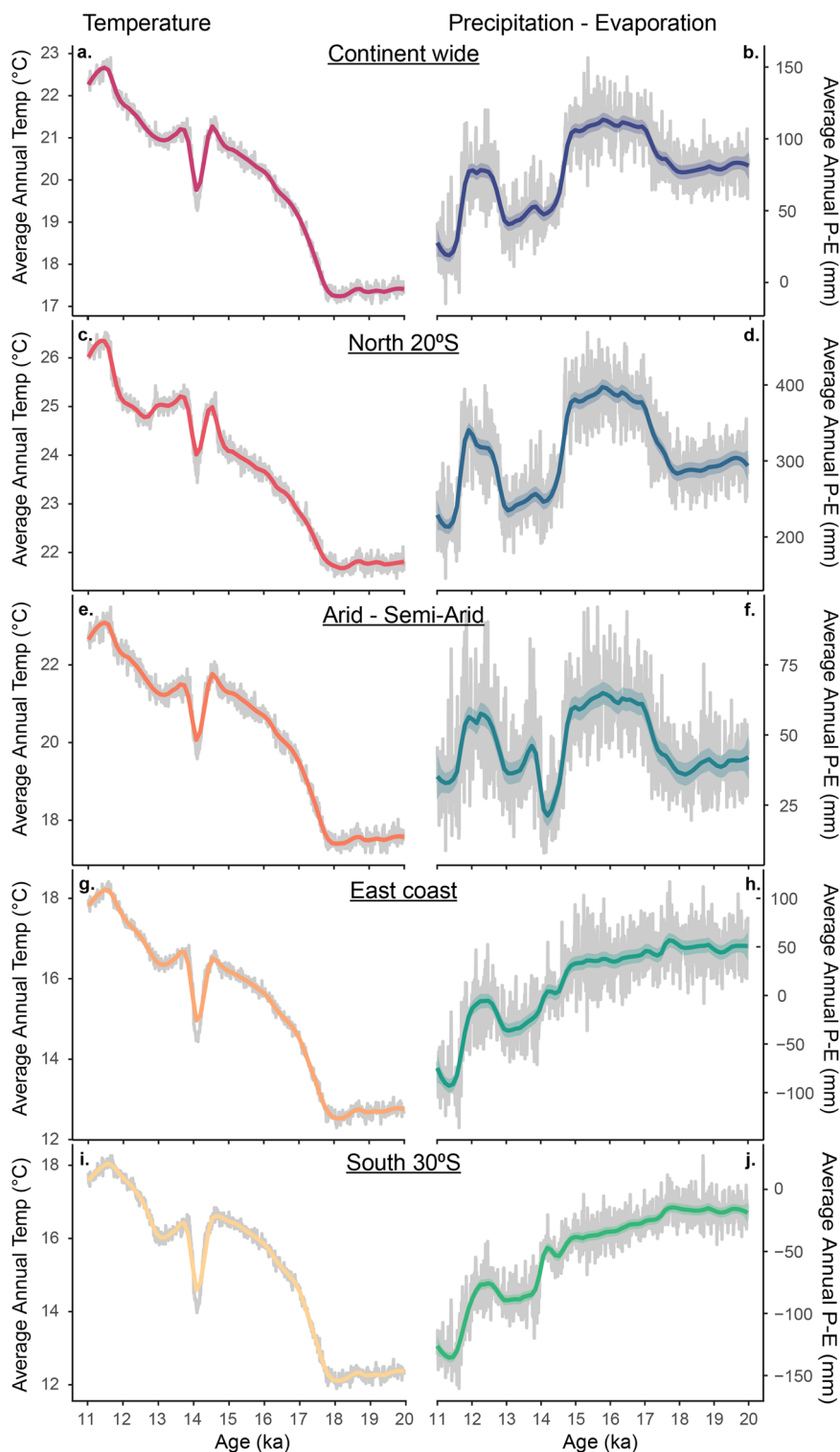
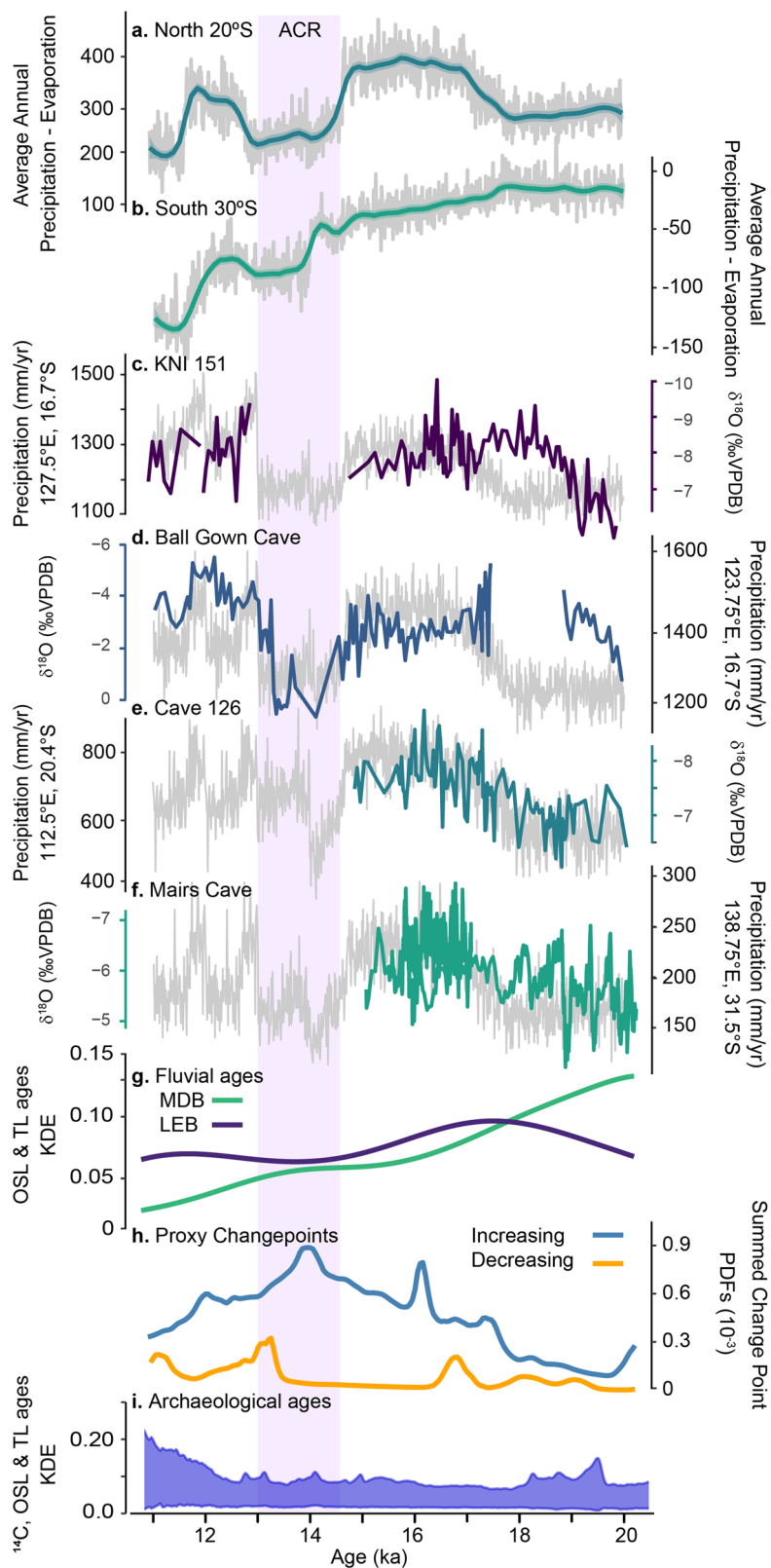


Fig. 3 iTrace decadal average annual temperature and moisture balance. iTrace decadal average annual temperature (**a, c, e, g, i**) and precipitation minus evaporation (P-E, **b, d, f, h, j**) from 20–11 ka averaged across all grid cells for (**a**) and (**b**). All continental cells, (**c**) and (**d**). Latitudes North of 20°S, (**e**) and (**f**). Arid - Semi-arid zone, (**g**) and (**h**). East coast continuous proxy record locations, (**i**) and (**j**). Latitudes South of 30°S. See Fig. S5 for grid cell locations.

temperatures, and moisture balance, reducing the resilience of arboreal vegetation communities whilst favouring switches to less woody vegetation communities. Interrogation of change points from pollen proxy records indicate that substantial changes in vegetation occur during the terminal Pleistocene (Fig. 4; Fig. S6). The increase in change points reflecting changes to greater arboreal vegetation occurs concurrently with a sustained increase in

temperature from 18.0 ka and CO₂ from 17.3 ka, whilst moisture balance remains stable. This suggests these changes in vegetation are responding to combined drivers of CO₂ and temperature, with more limited response to moisture balance. However, the trend towards increased arboreal vegetation declines during the ACR, in concert with declines in both temperature and moisture balance (Fig. S6). Change points to decreased arboreal vegetation are not



recorded during the ACR, suggesting that vegetation remained stable during this period. This may be the result of higher CO_2 values during the ACR compared to the LGM, or the short-lived nature of the ACR climate conditions.

Hesse et al.¹⁶ previously argued that even with lower precipitation, a reduction in evaporation and evapotranspiration loss,

driven by lower temperatures and reduced arboreal vegetation, would result in increased run-off, greater discharge volumes and larger river channels. The modelled P-E from the Lake Eyre and Murray-Darling Basins support this hypothesis, with both basins indicating positive moisture balance during the LGM and terminal Pleistocene. The modelled P-E shows strong coherence with

Fig. 4 iTRACE moisture balance and temperature with speleothem, fluvial and vegetation proxy data and kernel density estimate of

Archaeological data. **a, b** Decadal averaged iTRACE precipitation minus evaporation (P-E) averaged across all grid cells for a. Australian latitudes North of 20°S (see Fig. S5). **b** Australian latitudes South of 30°S (Fig. S5). **c-f** Decadal averaged iTRACE modelled precipitation (grey lines) from grid cell locations of Australian speleothem records from (c). KNI 151, (d). Ball Gown Cave, (e). Cave 126, (f). Mairs Cave (Fig. S2). Coloured lines represent $\delta^{18}\text{O}$ of calcite from each speleothem record. **g** KDEs of OSL and TL ages from all beach/shoreline, channel and overbank geomorphological features dated within the LEB (purple) and MDB (green) (Fig. S4). **h** Summed probability density function of all change points identified in vegetation, $\delta^{13}\text{C}$, $\delta^{18}\text{O}$ and GDGT records as representing a change to decreasing climate/vegetation indicators (including temperature, precipitation, and CO_2) (orange line) and all change points identified representing a change to increasing climate/vegetation indicators (including temperature, precipitation, and CO_2). **i** Gaussian KDE (bandwidth=30) of archaeological ages (radiocarbon, OSL & TL) through time.

the ages recorded from discontinuous fluvial features in both basins. The P-E values in the MDB suggest a long-term decline in moisture balance from 21 – 11 ka, in concert with proxy records.

We apply this improved understanding of the environmental conditions to archaeological records to explore human population dynamics during the terminal Pleistocene using the new SahulArch database⁶⁸. Kernel Density Estimates (KDEs) of all radiocarbon (^{14}C), optically stimulated luminescence (OSL) and thermoluminescence (TL) ages associated with archaeological material (minus replicate and superseded analyses) across the time period from 22 to 10 ka indicate broad stability in the number of ages (Fig. 2; Figs. S9–S15, see supplement for more details on methodology). A slight peak is evident between 20 and 18 ka, reflecting a focus of past research in the MDB during this temporal window (Figs. S9 and S10; ³²). The data does not indicate evidence of substantial changes in archaeological data between 21 and 11 ka. The KDE is remarkably consistent throughout the late LGM and terminal Pleistocene period, only beginning to show increases into the Holocene. The relative stability of archaeological ages over this 10,000-year period may suggest a stable population across Australia, with no evidence of large-scale population decline or collapse during this time.

A spatial re-organisation in sites is reflected in the archaeological data during the terminal Pleistocene, after 18 ka, possibly indicating different land use or activity across the landscape (Fig. 2; Fig. S9–S15). The late LGM is characterised by archaeological sites around the fringe of the continent, and in areas that coincide with the highest moisture balance, either in the monsoonal north, northwest rangelands or along the eastern seaboard (Fig. 2). With the exception of Tasmania, archaeological ages appear to be concentrated on major river systems fed by water from the northern rainfall systems, most evident in the north west^{69–71} and north central regions (Fig. 2; ^{30,52,53,72,73}). Notably, there are no archaeological ages recorded in extensive parts of the interior arid zone between 20 – 18 ka or in the LEB between 20 – 16 ka (Fig. 2; Figs. S9–S11), however this may be a function of sampling bias identified with use of the SahulArch database⁶⁸ and the reduced chance of site preservation in the low-elevation riverine and dune dominated environments. Given recent studies that suggest superhighways of movement through the arid interior during Marine Isotope Stage 3⁷⁴, this may suggest this zone was lesser used during the LGM and beginning of the terminal Pleistocene, rather than abandonment³⁸. This proposed reduced use is despite the modelled P-E across the arid – semi-arid interior being consistent with early Holocene values (Figs. 3 and S18), when the region is widely populated^{39,41,75,76}. As such, it may be demographic growth or socio-economic change in the Holocene that prompted the use of these interior environments, rather than behaviour driven solely by climatic conditions (Fig. 2; Fig. S16).

The large number of archaeological ages from Tasmania during the LGM and terminal Pleistocene is less clear but suggests the low temperatures during this period were not a barrier to human activity. Average annual temperatures were likely moderated by

maritime proximity during the LGM and would be considered adequate for human thermal comfort at $\sim 8^\circ\text{C}$. The majority of archaeological material is documented from the west coast^{77,78} where, although precipitation values were reduced by up to 300 mm/year, moisture balance was always positive and sufficient for human persistence in the region.

After the LGM, and particularly after 18 ka, the spread of human occupation appears to expand across large areas of the continent, coincident with increases in moisture balance and temperature (Fig. 2), yet the overall density of ages does not change. Two potential interpretations for the observed spatial patterning are: (1) an intensification of short term use of a large number of sites (point-to-point strategy) in response to dwindling resources⁴¹ as populations move more regularly through the landscape or, (2) improving resources that facilitated population spread and lengthier occupation in a given region, thereby leaving an increased archaeological signal^{49,79}. Given the timing of the spatial spread in concert with an increase in moisture balance, in particular across regions north of 20°S and the arid – semi-arid zone, the latter scenario seems more probable for most parts of the continent with the data reflecting increased residence times at individual sites across an ecologically ameliorating landscape. This pattern of occupation is more consistent with logistical mobility (establishing a base camp for a group, and then using a number of surrounding specialised satellite camps), technological strategies and settlement behaviour seen primarily in the late Holocene and ethnographically observed societies across Australia^{38,80–82}.

It is interesting to note that the ACR appears to play a substantial role in influencing Australia's climate (Fig. 3). Changes in temperature appear to be relatively short-lived, however P-E declines of up to 100 mm/yr are evident in some regions and are long lasting (up to 2000 years). All proxy records examined here indicate an influence of the ACR, although they are often cryptic in nature. Speleothem records from both Cave 126 and Mairs Cave terminate at the onset of the rainfall decline associated with the ACR, or immediately prior. In addition, the $\delta^{18}\text{O}$ record from KNI 151 indicates a growth hiatus during the ACR, while the Ball Gown Cave record shows a slow growth rate and isotopically high $\delta^{18}\text{O}$ across the ACR (Fig. 3), indicating reduced moisture availability. The ACR also coincides with a decline in fluvial geomorphic ages from the MDB⁸³ and a minimum in ages in the LEB (Fig. 4). Change points from continuous proxy records to higher proportions of arboreal vegetation peak during the ACR period before a decline and a slight increase in change points towards less arboreal vegetation (Fig. 4). This finding suggests that the ACR was a climatic period of similar conditions to the LGM, albeit shorter in duration, as recently suggested by Mooney et al.⁴⁶. Whilst substantially influencing continental climates, the ACR does not appear to have had an influence on the archaeological record (Fig. 4), however the influence of the ACR on human populations may be less obvious due to the limited temporal resolution and associated age uncertainty of the archaeological data used here.

Conclusion

Here we examined continental scale modelled temperature, precipitation and P-E data for Australia during the late LGM and terminal Pleistocene. Reinterpretation of published data and new data presented here provide a different perspective on long-standing ideas and concepts about the LGM in Australia. Most notably, evidence presented here suggests that the IASM did not collapse during the LGM and that regions north of 20°S experienced positive average annual moisture balance and higher than present day precipitation throughout this period. Our data suggests that the this northerly sourced moisture either directly or indirectly maintained hydrological systems fed from the north of the continent. Whilst summer precipitation in southern latitudes was slightly higher than present day during the LGM and much of the terminal Pleistocene, it was lower during winter and spring, perhaps reflecting a poleward contraction of the Southern Westerly Winds. Furthermore, although temperatures indicate the period was cooler, average continental values were on average only ~4 °C lower than present, with the higher latitudes showing the most substantive temperature decreases. We propose that reduced temperatures and CO₂ primarily led to the changes in key vegetation data from southern and eastern Australia that have previously been interpreted as an indication of extreme aridity. The ACR – a period that is rarely detected in Australian palaeoclimate research – appears to have been a key point of change in the broader continental climate and environments during the terminal Pleistocene.

We find no substantive change in the frequency of archaeological ages between 20 – 12 ka. Archaeological age data density during the peak LGM is greatest in Tasmania, coastal regions, along major river systems in the northwest rangelands and the MDB. The archaeological data suggests reduced use, but not absence, of the arid centre until after 18 ka. This revised view of continued population numbers, albeit with a decline in spatial utilisation, aligns more closely with archaeological and genomic records, that do not suggest large-scale population change, abandonment, or mass migration after the initial peopling of most regions >40,000 years ago.

With our improved understanding of the palaeoclimate record, some LGM palaeoenvironmental and archaeological archives may need to be revisited and, in some instances, reconsidered. We demonstrate that on such a large continent, there is increasingly complexity in the data, and simplified models – notably in human behaviour – cannot robustly explain all observations. While researchers continue to develop continental scale interpretations, further regional and local level of investigation and interrogation is needed to provide their foundation. Finally, our data continues to demonstrate the importance of the terminal Pleistocene for Aboriginal societies and their adaption to change, suggesting a far greater agency in the occupation and movement across Australia, irrespective of environmental conditions.

Materials and methods

The iTRACE utilises the Community Earth System Model (CESM) version 1.3 with fully coupled water isotope ($\delta^{18}\text{O}$ and δD) modules (iCESM) in the atmosphere, ocean, land, sea ice and river runoff components⁸⁴. Precipitation (mm/day) combines the large-scale (stable) precipitation rate (including both liquid and ice; mm/day) and convective precipitation rate (including both liquid and ice; mm/day). The temperature output represents the radiative surface temperature (TS; degree Celsius; °C). Evaporation is the total surface water flux, including evaporation plus transpiration (mm/day), with P-E the Precipitation minus Evaporation. Simulations are presented from time slices at 20, 18, 16, 14, 13.5, 12.5 and 11 ka. Model outputs from the same grid cells were compared

to $\delta^{18}\text{O}$ of calcite from Australian speleothem records obtained from the Speleothem Isotope Synthesis and Analyses (SISAL) database (Figure S2, S3; ⁸⁵). A Kernel Density Estimation (KDE) was determined from optically stimulated luminescence (OSL) and thermo luminescence (TL) ages from lacustrine beach and shoreline ages and fluvial overbank and channel ages was from the two largest river systems in Australia, the Murray Darling Basin, and the Lake Eyre Basin (Figure S1). Discontinuous archive ages were accessed from the OCTOPUS database v.2 (<https://octopusdata.org/>)⁸⁶. Continuous lacustrine proxy records ($n = 35$) were analyzed for the period 22 – 8ka using the same methodology as Cadd et al.⁵. Model outputs, supported by palaeoenvironmental proxy records, were examined in relation to radiocarbon (¹⁴C), OSL and TL ages associated with archaeological artefacts and deposits from the SahulArch V2 database⁶⁸. For detailed description and full methods see Supplement.

Data availability

iTRACE climate simulation data is available at <https://www.earthsystemgrid.org/dataset/ucar.cgd.cesm4.iTRACE.html>. Speleothem records are available at <https://doi.org/10.17864/1947.256>. Discontinuous proxy records and Archaeological data are available at <https://octopusdata.org/>. Modern precipitation and temperature data are available via the Australian Bureau of Meteorology (BOM) <http://www.bom.gov.au/climate/data/>. Additional data supporting these findings are archived at Zenodo <https://zenodo.org/records/10360104>.

Code availability

The code related to the analyses are available at <https://zenodo.org/records/10360104>.

Received: 14 June 2023; Accepted: 4 January 2024;

Published online: 25 January 2024

References

- Turney, C. et al. Integration of ice-core, marine and terrestrial records for the Australian Last Glacial Maximum and Termination: a contribution from the OZ INTIMATE group. *J. Quat. Sci.* **21**, 751–761 (2006).
- Hesse, P. P. The record of continental dust from Australia in Tasman Sea Sediments. *Quat. Sci. Rev.* **13**, 257–272 (1994).
- Miller, G. H., Magee, J. W. & Jull, A. J. T. Low-latitude glacial cooling in the Southern Hemisphere from amino-acid racemization in emu eggshells. *Nature* **385**, 241–244 (1997).
- Magee, J. W. & Miller, G. H. Lake Eyre palaeohydrology from 60 ka to the present: Beach ridges and glacial maximum aridity. *Palaeogeogr. Palaeoclimatol. Palaeoecol.* **144**, 307–329 (1998).
- Cadd, H. et al. A continental perspective on the timing of environmental change during the last glacial stage in Australia. *Quat. Res.* **102**, 5–23 (2021).
- Donders, T. H., Wagner, F. & Visscher, H. Late Pleistocene and Holocene subtropical vegetation dynamics recorded in perched lake deposits on Fraser Island, Queensland, Australia. *Palaeogeogr. Palaeoclimatol. Palaeoecol.* **241**, 417–439 (2006).
- Harrison, S. P. Late Quaternary lake-level changes and climates of Australia. *Quat. Sci. Rev.* **12**, 211–231 (1993).
- Builth, H. et al. Environmental and cultural change on the Mt Eccles lava-flow landscapes of southwest Victoria, Australia. *Holocene* **18**, 413–424 (2008).
- Dodson, J. R. Vegetation history and water fluctuations at lake leake, South-Eastern South Australia. II.* 50 000 B.P. To 10 000 B.P. *Aust. J. Bot.* **23**, 815–831 (1975).
- Harle, K. J. Late Quaternary vegetation and climate change in southeastern Australia: Palynological evidence from marine core E55-6. *Palaeogeogr. Palaeoclimatol. Palaeoecol.* **131**, 465–483 (1997).
- Colhoun, E. A., Pola, J. S., Barton, C. E. & Heijnis, H. Late Pleistocene vegetation and climate history of Lake Selina, western Tasmania. *Quat. Int* **57–58**, 5–23 (1999).
- Kershaw, A. P. et al. A high-resolution record of vegetation and climate through the last glacial cycle from Caledonia Fen, southeastern highlands of Australia. *J. Quat. Sci.* **22**, 801–815 (2007).
- Petherick, L., McGowan, H. & Moss, P. Climate variability during the Last Glacial Maximum in eastern Australia: Evidence of two stadials? *J. Quat. Sci.* **23**, 787–802 (2008).

14. Treble, P. C. et al. Hydroclimate of the Last Glacial Maximum and deglaciation in southern Australia's arid margin interpreted from speleothem records (23–15 ka). *Clim. Past* **13**, 667–687 (2017).
15. Denniston, R. F. et al. North Atlantic forcing of millennial-scale Indo-Australian monsoon dynamics during the Last Glacial period. *Quat. Sci. Rev.* **72**, 159–168 (2013).
16. Hesse, P. P. et al. Palaeohydrology of lowland rivers in the Murray-Darling Basin, Australia. *Quat. Sci. Rev.* **200**, 85–105 (2018).
17. Mueller, D. et al. Revisiting an arid LGM using fluvial archives: a luminescence chronology for palaeochannels of the Murrumbidgee River, south-eastern Australia. *J. Quat. Sci.* **33**, 777–793 (2018).
18. Reinfelds, I., Swanson, E., Cohen, T., Larsen, J. & Nolan, A. Hydrospatial assessment of streamflow yields and effects of climate change: Snowy Mountains, Australia. *J. Hydrol.* **512**, 206–220 (2014).
19. Page, K. J., Kemp, J. & Nanson, G. C. Late Quaternary evolution of Riverine plain paleochannels, southeastern Australia. *Aust. J. Earth Sci.* **56** (2009).
20. Barrows, T. T. et al. Late Pleistocene lake level history of Lake Mungo, Australia. *Quat. Sci. Rev.* **238**, 106338 (2020).
21. Kemp, J. & Rhodes, E. J. Episodic fluvial activity of inland rivers in southeastern Australia: Palaeochannel systems and terraces of the Lachlan River. *Quat. Sci. Rev.* **29**, 732–752 (2010).
22. Petherick, L. et al. Climatic records over the past 30ka from temperate Australia - a synthesis from the Oz-INTIMATE workgroup. *Quat. Sci. Rev.* **74**, 58–77 (2013).
23. Fitzsimmons, K. E., Stern, N., Murray-Wallace, C. V., Truscott, W. & Pop, C. The Mungo mega-lake event, semi-arid Australia: Non-linear descent into the last ice age, implications for human behaviour. *PLoS One* **10**, 1–19 (2015).
24. Fitzsimmons, K. E. et al. Late Quaternary palaeoenvironmental change in the Australian drylands. *Quat. Sci. Rev.* **74**, 78–96 (2013).
25. Haberlah, D. et al. Loess and floods: High-resolution multi-proxy data of Last Glacial Maximum (LGM) slackwater deposition in the Flinders Ranges, semi-arid South Australia. *Quat. Sci. Rev.* **29**, 2673–2693 (2010).
26. Petherick, L. M. et al. An extended last glacial maximum in the Southern Hemisphere: A contribution to the SHeMax project. *Earth-Science Rev.* **231**, 104090 (2022).
27. Du, Y., Brown, J. R. & Sniderman, J. M. K. Last glacial maximum climate and atmospheric circulation over the Australian region from climate models. *Clim. Past Discuss.* 1–34 (2023).
28. D'Costa, D. M., Edney, P., Kershaw, A. P. & De Deckker, P. Late quaternary palaeoecology of Tower Hill, Victoria, Australia. *J. Biogeogr.* **16**, 461–482 (1989).
29. Prentice, I. C., Cleator, S. F., Huang, Y. H., Harrison, S. P. & Roulstone, I. Reconstructing ice-age palaeoclimates: Quantifying low-CO₂ effects on plants. *Glob. Planet. Change* **149**, 166–176 (2017).
30. Prentice, I. C., Villegas-Diaz, R. & Harrison, S. P. Accounting for atmospheric carbon dioxide variations in pollen-based reconstruction of past hydroclimates. *Glob. Planet. Change* **211**, 103790 (2022).
31. Martin Calvo, M. & Prentice, I. C. Effects of fire and CO₂ on biogeography and primary production in glacial and modern climates. *New Phytol.* **208**, 987–994 (2015).
32. Cowling, S. A. & Sykes, M. T. Physiological significance of low atmospheric CO₂ for Plant–Climate Interactions. *Quat. Res.* **52**, 237–242 (1999).
33. Scheff, J., Seager, R., Liu, H. & Coats, S. Are glacials dry? Consequences for paleoclimatology and for greenhouse warming. *J. Clim.* **30**, 6593–6609 (2017).
34. O'Connor, S., Veth, P. & Hubbard, N. "Changing interpretations of postglacial human subsistence and demography in Sahul" in *Sahul in Review: The Archaeology of Australia, New Guinea and Island Melanesia*, (The Australian National University, 1993), pp. 95–105.
35. Hiscock, P. & Wallis, L. A. *Pleistocene settlement of deserts from an Australian perspective* (Blackwell Oxford, 2005).
36. Hiscock, P. Prehistoric settlement patterns and artefact manufacture at Lawn Hill. *Northwest Queensl. [dissertation] Univ. Queensl.* (1989).
37. Veth, P. Islands in the interior: a model for the colonization of Australia's arid zone. *Archaeol. Ocean.* **24**, 81–92 (1989).
38. Veth, P., McDonald, J. & Hiscock, P. "Beyond the Barriers: A New Model for the Settlement of Australian Deserts" in *The Oxford Handbook of the Archaeology of Indigenous Australia and New Guinea*, I. J. McNiven, B. David, Eds. (Oxford University Press, 2022), p. 0.
39. Williams, A. N. A new population curve for prehistoric Australia. *Proc. R. Soc. B Biol. Sci.* **280**, 20130486 (2013).
40. Petherick, L. M., Moss, P. T. & McGowan, H. A. An extended Last Glacial Maximum in subtropical Australia. *Quat. Int.* **432**, 1–12 (2017).
41. Smith, M. *The archaeology of Australia's deserts* (Cambridge University Press, 2013).
42. Tobler, R. et al. Aboriginal mitogenomes reveal 50,000 years of regionalism in Australia. *Nature* **544**, 180–184 (2017).
43. Bergström, A. et al. Deep roots for aboriginal Australian Y chromosomes. *Curr. Biol.* **26**, 809–813 (2016).
44. Nagle, N. et al. Mitochondrial DNA diversity of present-day Aboriginal Australians and implications for human evolution in Oceania. *J. Hum. Genet.* **62**, 343–353 (2017).
45. Pedro, J. B. et al. The spatial extent and dynamics of the Antarctic Cold Reversal. *Nat. Geosci.* **9**, 51–55 (2016).
46. Mooney, S., Martin, L., Goff, J. & Young, A. R. M. Sedimentation and organic content in the mires and other sites of sediment accumulation in the Sydney region, eastern Australia, in the period after the Last Glacial Maximum. *Quat. Sci. Rev.* **272**, 107216 (2021).
47. Moss, P. T., Tibby, J., Petherick, L., McGowan, H. & Barr, C. Late Quaternary vegetation history of North Stradbroke Island, Queensland, eastern Australia. *Quat. Sci. Rev.* **74**, 257–272 (2013).
48. Li, T. et al. Environmental change inferred from multiple proxies from an 18 cal ka BP sediment record, Lake Barrine, NE Australia. *Quat. Sci. Rev.* **294**, 107751 (2022).
49. Williams, A. N. et al. A continental narrative: Human settlement patterns and Australian climate change over the last 35,000 years. *Quat. Sci. Rev.* **123**, 91–112 (2015).
50. Barrows, T. T., Mills, S. C., Fitzsimmons, K., Wasson, R. & Galloway, R. Low-altitude periglacial activity in southeastern Australia during the late Pleistocene. *Quat. Res. (United States)* **107**, 125–146 (2022).
51. Woltering, M. et al. Glacial and Holocene terrestrial temperature variability in subtropical east Australia as inferred from branched GDGT distributions in a sediment core from Lake McKenzie. *Quat. Res.* **82**, 132–145 (2014).
52. Chang, J. C. et al. A chironomid-inferred summer temperature reconstruction from subtropical Australia during the last glacial maximum (LGM) and the last deglaciation. *Quat. Sci. Rev.* **122**, 282–292 (2015).
53. Kageyama, M. et al. The PMIP4 Last Glacial Maximum experiments: Preliminary results and comparison with the PMP3 simulations. *Clim. Past* **17**, 1065–1089 (2021).
54. He, C. et al. Hydroclimate footprint of pan-Asian monsoon water isotope during the last deglaciation. *Sci. Adv.* **7**, 1–12 (2021).
55. Buckingham, F. L. et al. Termination 1 millennial-scale rainfall events over the Sunda shelf. *Geophys. Res. Lett.* **49**, 1–10 (2022).
56. Marshall, A. G. & Lynch, A. H. The sensitivity of the Australian summer monsoon to climate forcing during the late Quaternary. *J. Geophys. Res. Atmos.* **113**, 1–12 (2008).
57. Marshall, A. G. & Lynch, A. H. Time-slice analysis of the Australian summer monsoon during the late Quaternary using the Fast Ocean Atmosphere. *Model. J. Quat. Sci.* **21**, 789–801 (2006).
58. De Deckker, P., Barrows, T. T. & Rogers, J. Land-sea correlations in the Australian region: Post-glacial onset of the monsoon in northwestern Western Australia. *Quat. Sci. Rev.* **105**, 181–194 (2014).
59. Wyrwoll, K. H. & Miller, G. H. Initiation of the Australian summer monsoon 14,000 years ago. *Quat. Int.* **82**, 119–128 (2001).
60. Ayliffe, L. K. et al. Rapid interhemispheric climate links via the Australasian monsoon during the last deglaciation. *Nat. Commun.* **4**, 1–6 (2013).
61. Muller, J., McManus, J. F., Oppo, D. W. & Francois, R. Strengthening of the Northeast Monsoon over the Flores Sea, Indonesia, at the time of Heinrich event 1. *Geology* **40**, 635–638 (2012).
62. Dwi Wahyu Ardi, Ryan et al. Last deglaciation - holocene Australian-Indonesian monsoon rainfall changes off Southwest Sumba, Indonesia. *Atmosphere (Basel)* **11**, 932 (2020).
63. Denniston, R. F. et al. A Last Glacial Maximum through middle Holocene stalagmite record of coastal Western Australia climate. *Quat. Sci. Rev.* **77**, 101–112 (2013).
64. Denniston, R. F. et al. Decoupling of monsoon activity across the northern and southern Indo-Pacific during the Late Glacial. *Quat. Sci. Rev.* **176**, 101–105 (2017).
65. Yan, M., Wang, B. & Liu, J. Global monsoon change during the Last Glacial Maximum: a multi - model study. *Clim. Dyn.* **47**, 359–374 (2016).
66. Yan, M. et al. Understanding the Australian Monsoon change during the Last Glacial Maximum with a multi-model ensemble. *Clim. Past* **14**, 2037–2052 (2018).
67. Meneghini, B., Simmonds, I. & Smith, I. N. Association between Australian rainfall and the Southern Annular Mode. *Int. J. Climatol.* **27**, 109–121 (2007).
68. Saktura, W. M. et al. SahulArch: A geoarchaeological database for the archaeology of Sahul. *Aust. Archaeol.* 1–13 (2023).
69. Slack, M., Fillios, M. & Fullagar, R. Aboriginal settlement during the LGM at Brockman, Pilbara region, Western Australia. *Archaeol. Ocean.* **44**, 32–39 (2009).
70. Veth, P., Ward, I. & Ditchfield, K. Reconceptualising Last Glacial Maximum discontinuities: A case study from the maritime deserts of north-western Australia. *J. Anthropol. Archaeol.* **46**, 82–91 (2017).
71. Marwick, B. Milly's Cave: Evidence for Human Occupation of the Inland Pilbara during the Last Glacial Maximum. *Tempus* **7**, 21–33 (2002).
72. Slack, M. J. "Between the desert and the Gulf: evolutionary anthropology and Aboriginal prehistory in the Riversleigh/Lawn Hill region, Northern Australia," University of Sydney. (2007).

73. Wallis, L. A., Keys, B., Moffat, I. & Fallon, S. Gledswood shelter 1: Initial radiocarbon dates from a Pleistocene aged Rockshelter site in Northwest Queensland. *Aust. Archaeol* **69**, 71–74 (2009).
74. Crabtree, S. A. et al. Landscape rules predict optimal superhighways for the first peopling of Sahul. *Nat. Hum. Behav.* **5**, 1303–1313 (2021).
75. Smith, M. A., Williams, A. N., Turney, C. S. M. & Cupper, M. L. Human-environment interactions in Australian drylands: Exploratory time-series analysis of archaeological records. *Holocene* **18**, 389–401 (2008).
76. Ulm, S. Complexity and the Australian continental narrative: Themes in the archaeology of Holocene Australia. *Quat. Int.* **285**, 182–192 (2013).
77. Cosgrove, R. & Pleistocene, Late behavioural variation and time trends: the case from Tasmania. *Archaeol. Ocean.* **30**, 83–104 (1995).
78. Stern, N. & Allen, J. “Pallawa Trounta shelter” (La Trobe University Melbourne, 1996).
79. Bird, D. W. & O’Connell, J. F. Behavioral ecology and archaeology. *J. Archaeol. Res.* **14**, 143–188 (2006).
80. Gould, R.A. *Yiwara: foragers of the Australian desert* (HarperCollins, 1969).
81. Cane, S. *Desert demography: A case study of pre-contact Aboriginal densities in the Western Desert of Australia* (1990).
82. Long, J. P. M. “Arid region aborigines: the Pintubi” in *Aboriginal Man in Australia*, D. Mulvaney, J. Golson, Eds. (The Australian National University, 1967), pp. 262–270.
83. De Deckker, P., Moros, M., Perner, K. & Jansen, E. Influence of the tropics and southern westerlies on glacial interhemispheric asymmetry. *Nat. Geosci.* **5**, 266–269 (2012).
84. Brady, E. et al. The connected isotopic water cycle in the community earth system model version 1. *J. Adv. Model. Earth Syst.* **11**, 2547–2566 (2019).
85. Comas-Bru, L. et al. SISALv2: A comprehensive speleothem isotope database with multiple age-depth models. *Earth Syst. Sci. Data* **12**, 2579–2606 (2020).
86. Codilean, A. T. et al. OCTOPUS database (v.2). *Earth Syst. Sci. Data* **14**, 3695–3713 (2022).
87. Evans, A., Jones, D., Smalley, R. & Lelleyett, S. An enhanced gridded rainfall analysis scheme for Australia. *Aust. Bur. Meteorol. Melbourne, VIC, Aust.* **66**, 55–67 (2020).

Acknowledgements

We wish to acknowledge the long connection to Country held by the First Nations peoples of Australia, who are the first custodians of this Country. This work was supported by the ARC Centre of Excellence for Australian Biodiversity and Heritage (CABAH, Project Number CE170100015). We would like to thank the members of the CABAH LGM Workshop at UNSW in 2019, in particular the late Lynda Petherick. The CESM project is supported primarily by the NSF. This material is based on work supported by the National Centre for Atmospheric Research, which is a major facility sponsored by the NSF under Cooperative Agreement no. 1852977. Computing and data

storage resources, including the Cheyenne supercomputer (<https://doi.org/10.5065/D6RX99HX>), were provided by the Computational and Information Systems Laboratory (CISL) at NCAR.

Author contributions

Conceptualisation: H.C., A.N.W., C.S.M.T., T.J.C., S.D.M.; Research design: H.C.; Analysis: H.C., A.N.W.; Writing—H.C., A.N.W.; Writing—review & editing: W.S., C.H., B.O.B., T.J.C., S.D.M., C.S.M.T. All authors gave final approval for publication.

Competing interests

The authors declare no competing interests.

Additional information

Supplementary information The online version contains supplementary material available at <https://doi.org/10.1038/s43247-024-01204-1>.

Correspondence and requests for materials should be addressed to Haidee Cadd.

Peer review information *Communications Earth & Environment* thanks Pauline Treble, Peter Veth and the other, anonymous, reviewer(s) for their contribution to the peer review of this work. Primary Handling Editors: Ola Kwiciec and Aliénor Lavergne. A peer review file is available.

Reprints and permission information is available at <http://www.nature.com/reprints>

Publisher’s note Springer Nature remains neutral with regard to jurisdictional claims in published maps and institutional affiliations.



Open Access This article is licensed under a Creative Commons Attribution 4.0 International License, which permits use, sharing, adaptation, distribution and reproduction in any medium or format, as long as you give appropriate credit to the original author(s) and the source, provide a link to the Creative Commons licence, and indicate if changes were made. The images or other third party material in this article are included in the article’s Creative Commons licence, unless indicated otherwise in a credit line to the material. If material is not included in the article’s Creative Commons licence and your intended use is not permitted by statutory regulation or exceeds the permitted use, you will need to obtain permission directly from the copyright holder. To view a copy of this licence, visit <http://creativecommons.org/licenses/by/4.0/>.

© The Author(s) 2024